JOURNAL OF COMPUTATIONAL PHYSICS 58, 80–95 (1985)

# Numerical Simulation of Nonstationary Processes in Free Electron Lasers

YA. L. BOGOMOLOV AND A. D. YUNAKOVSKY

*Institute of Applied Physics of the Academy of Sciences USSR, 603600 Gorky, USSR*

Received March 3, 1983; revised April 17, 1984

A computational scheme is developed to integrate a set of self-consistent equations describing the evolution of the field structure in free electron lasers. The proposed scheme is fourth-order accurate in space and third-order accurate in time. The boundedness of solution is provided by a number of integrals in the scheme. Stationary and pulse electron injection regimes are investigated. In both cases the scheme permits effective calculation of the following regimes: (a) stationary single-mode generation (or, correspondingly, generation of identical pulses), (b) periodic self-modulation, (c) stochastic self-modulation. 

## 1. INTRODUCTION

One of the most complicated problems of the numerical simulation of the interaction between electromagnetic waves and relativistic particle beams in free electron lasers (FELs) is the investigation of nonstationary multifrequency generation processes. An important feature of FELs is that the dimensions of their electrodynamic systems are much larger than the wavelength, so, the amplification band contains a large number of eigenfrequencies, which, as a rule, are quasi-equidistant. Thus, in the Stanford infrared FEL [1] the number of amplified modes was $\sim 10^4$. To describe the evolution of the amplitudes of these modes within the framework of the mode approach [2], the number of equations of the same order is necessary. Meanwhile, since the period of the current pulse sequence is close to the period of the wave pass through the cavity, the phases of modes are locked and their amplitudes are correlated so that the modes compose a slowly evolving wave packet. Therefore, it is sufficient to keep an eye on several tens of points given on the packet length in terms of the space–time approach and it is no wonder that this method was preferred in the most of papers [3–8].

In its direct form this approach requires the calculation of the interaction between electrons and a synchronous wave for each wave pass through the cavity [5–6]. Such a simulation is very effective, if the radiation losses are rather high for a pass. However, if the radiation losses decrease and, consequently, the mirror reflection coefficients $R_{1,2}$ tend to unity (the case of a high-quality cavity), a large number of



0021-9991/85 $3.00

passes ($\sim 1/(1 - R_1 \cdot R_2)$) is needed for oscillations to set up. In such a situation, taking into consideration small variations of the wave amplitude for one pass through the cavity, it is reasonable to change the discrete variable $n$ (the number of the pass) by the continuous variable $\tau$ (slow time) [7]. Then the time integration step $\Delta\tau$ will correspond to $\Delta n = \Delta\tau/(1 - R_1 \cdot R_2)$ real wave passes and the closer to unity the reflection coefficients, the greater the advantages of the method proposed in [7] than that in [5, 6] (e.g., in the Stanford experiment [1] $R_1 \cdot R_2 \simeq 0.965$ and $\Delta n/\Delta\tau \simeq 30$).

Besides, a considerable decrease of the time of computation can be achieved by optimization of the time-consuming procedure—integration of the electron motion equation (generalized pendulum equation). For this purpose we have used a new numerical algorithm [9] (see Sect. 3), having a number of advantages compared with the standard technique (few computation operations for one integration step, a high order of an accuracy, the presence of some numerical integrals that provide boundedness of solution) which enables one to use larger computation steps. This algorithm can be recommended also for calculation of FELs with low-reflection mirrors and, consequently, with high pulse amplification for one pass. In particular, it has been used for the numerical simulation of FELs with a distributed feedback [10].

The scheme of computation as a whole was a very effective one for investigation of FELs both with pulse and stationary electron injection and permitted us to study the regimes of stationary generations as well as the regimes of periodic and stochastic self-modulation (see [8] and Sect. 4).

## 2. The Differential Equations

For FEL-generators with high-reflection mirrors and, consequently, with low wave amplification for one pass the equations of wavebeam interaction in the case of stationary electron injection have the form [7, 8]

$$\frac{\partial A}{\partial \tau} + A = \int_0^L I \, dz, \tag{1}$$

$$\left(\frac{\partial}{\partial x} + \frac{\partial}{\partial z}\right)^2 \theta = \mathrm{Re}(A e^{i\theta}). \tag{2}$$

Initial and boundary conditions are given by

$$\theta/_{z=0} = \theta_0 \in [0, 2\pi], \qquad \left(\frac{\partial}{\partial x} + \frac{\partial}{\partial z}\right) \theta/_{z=0} = \delta \tag{3}$$

for electrons and

$$A(x, \tau = 0) = A_0(x), \tag{4a}$$

$$A(x, \tau) = A(x + T_r, \tau) \tag{4b}$$

for the wave, Here $A(x, \tau)$ is the slowly varying wave amplitude, $\theta_0$ and $\theta$ the initial and current phases of electrons with respect to the wave, $I(x, z, \tau) = (1/2\pi)\int_0^{2\pi} e^{-i\theta}\, d\theta_0$ the electron current harmonic synchronous to the wave, $L$ the dimensionless length of wavebeam interaction space, $T_r$ the wave reversal period, $\delta$ the initial mismatch of synchronism between electrons and the wave.

In the case of pulse injection [1] the electron motion equation (2) and the initial conditions (3) remain unchanged, while the equation for the wave (1) is modified [7, 8],

$$\frac{\partial A}{\partial \tau} - \varepsilon \frac{\partial A}{\partial x} + A = \int_0^L g(x - z) I\, dz, \tag{5}$$

where

$$\begin{aligned} g(x - z) &= 1, \qquad 0 \leqslant x - z \leqslant T_c, \\ &= 0, \qquad x - z \leqslant 0,\ x - z \geqslant T_c \end{aligned}$$

$\varepsilon$ is the tact synchronism mismatch; $T_c$ is the pulse sequence period. In its turn, the boundary condition (4b) is changed by

$$A(\tau, L + T_c) = 0.$$

The dimensionless efficiency of the FEL is given by [8]

$$\eta(\tau) = \frac{1}{2\pi T_c} \int_L^{T_c + L} dx \int_0^{2\pi} \left( \frac{\partial}{\partial z} + \frac{\partial}{\partial x} \right) \theta /_{z=L}\, d\theta_0. \tag{6}$$

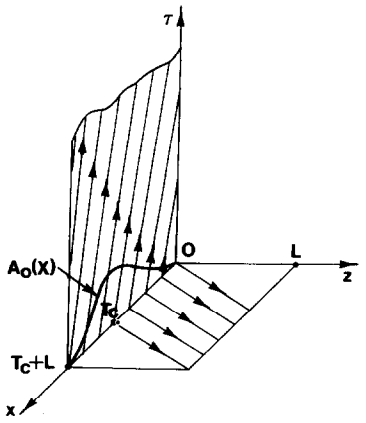


FIG. 1. Characteristics of the equation for the wave in the plane $x$, $\tau$ and electron motion equation characteristics in the plane $x$, $z$ in the case of pulse electron injection.

To visualize the given equations Fig. 1 displays the characteristics of Eq. (5) in the plane $x$, $\tau$ and the characteristics of Eq. (2) in the plane $x$, $z$. Note that the characteristics of Eq. (1) (the case of stationary electron injection) are parallel to the $\tau$ axis.

Using the specific form of Eqs. (1), (2) (or (1), (5)), one can apply the following splitting procedure. At the given time level $\tau = \tau_0$, assuming that $A(x, \tau_0)$ is known, we first numerically integrate the electron motion equation (2), then calculate $\int_0^L I\, dz$, that, in its turn, permits us to execute one time step in Eq. (1) (or (5)). Thus, the problem of the numerical scheme designing for the electron motion equation can be considered independent of that for the equation for the wave.

## 3. Numerical Integration of the Electron Motion Equation

We introduce a rectangular uniform grid in the plane $x$, $z$ with a mesh size in $x$ coordinate equal to that in $z$ coordinate. The necessity of $x$ and $z$ mesh size equality is explained by the wave amplitude values $A$ which are known only at the grid points, while the electron motion equation should be integrated along the characteristics whose direction is labeled by $l$.

Introduction of $\theta_0$ variable discreteness (the use of the method of large particles for the electron beam simulation) reduces the initial problem to the solving of $N \times N_1$ independent ordinary differential equations

$$2\frac{\partial^2 \theta_{k,m}}{\partial l^2} = \mathrm{Re}(Ae^{i\theta_{k,m}}),$$
$$\theta_{k,m}|_{z=0} = \frac{2\pi(k-1)}{N}, \qquad \left.\frac{\partial \theta_{k,m}}{\partial l}\right|_{z=0} = \delta_k, \qquad k = \overline{1, N},\ m = \overline{1, N_1}, \tag{7}$$

where $N$ is the number of macroparticles moving along one and the same trajectory, $N_1$ the number of trajectories (the number of grid points in $x$ coordinate).

Later on, $k$ and $m$ indices will be omitted (we shall consider only one equation for the fixed $k$ and $m$) and the points will mean differentiation with respect to $l$. Besides, $h$ will denote a mesh size in $x$ and $z$ coordinates, while $\Delta l = \sqrt{2}\, h$ will be an integration step along the characteristics.

Since the right-hand sides of Eqs. (1), (2), (5) contain the $\theta$ variable only as an argument of exponents, it is natural to introduce the new unknown variable $\varphi = \varphi_1 + i\varphi_2 = e^{i\theta}$. Then Eq. (7) becomes

$$\ddot{\varphi} - \dot{\varphi}^2 \varphi^* - \tfrac{1}{2} i\varphi\, \mathrm{Re}(A\varphi) = 0 \qquad (\varphi^* = e^{-i\theta}),$$
$$\varphi(0) = e^{i(2\pi(k-1)/N)}, \qquad \dot{\varphi}(0) = i\delta_k \varphi(0).$$

The latter, in its turn, is equivalent to the following set of equations

$$\dot{\varphi}_1 = \psi_1,$$
$$\dot{\varphi}_2 = \psi_2,$$
$$\dot{\psi}_1 = -\varphi_1(\psi_1^2 + \psi_2^2) - \tfrac{1}{2}\varphi_2(A_1\varphi_1 - A_2\varphi_2),$$
$$\dot{\psi}_2 = -\varphi_2(\psi_1^2 + \psi_2^2) + \tfrac{1}{2}\varphi_1(A_1\varphi_1 - A_2\varphi_2), \tag{8}$$

$$\varphi_1(0) = \cos\frac{2\pi(k-1)}{N}, \qquad \varphi_2(0) = \sin\frac{2\pi(k-1)}{N},$$
$$\psi_1(0) = -\delta_k\varphi_2(0), \qquad \psi_2(0) = \delta_k\varphi_1(0),$$
$$A_1 = \mathrm{Re}(A), \qquad A_2 = \mathrm{Im}(A).$$

This set of equations can be inregrated by some standard technique. Two evident integrals of the the set (8) can be used to check the correctness of calculations

$$\varphi_1^2 + \varphi_2^2 = 1, \tag{9a}$$
$$\varphi_1\psi_1 + \varphi_2\psi_2 = 0. \tag{9b}$$

Note that there is a solution correction procedure given later which ensures precisely the relationship (9a) (that provides boundedness of solution with respect to $\varphi_1$ and $\varphi_2$) and decreases the truncation error. But such a procedure is absent for the integral (9b). Moreover, the structure of this integral allows the large values of $\psi_1$ and $\psi_2$. Besides, when $\varphi_1 \sim 1$ ($\varphi_2 \sim 0$) or $\varphi_2 \sim 1$ ($\varphi_1 \sim 0$) one may expect the appearance of an explosive instability such as $1/(t - t_0)$ usual for the equation $\dot{\psi} = \psi^2$. The above-mentioned considerations are not in favor of such a simple approach to the solving of Eq. (7).

We now twice integrate Eq. (7) over the interval $[0, \Delta l]$ (symbol $\vee$ denotes variables at the initial point of the characteristic and symbol $\wedge$ at the calculated point)

$$\hat{\theta} = \check{\theta} + \tfrac{1}{2}\int_0^{\Delta l} \mathrm{Re}(Ae^{i\theta})\, dl,$$

$$\hat{\theta} = \check{\theta} + \check{\dot{\theta}}\Delta l + \tfrac{1}{2}\int_0^{\Delta l} (\Delta l - l)\,\mathrm{Re}(Ae^{i\theta})\, dl,$$

and set

$$U + iV = e^{i\theta}, \tag{10a}$$
$$\varphi + i\psi = e^{i\dot{\theta}\Delta l}. \tag{10b}$$

Then

$$\hat{U} + i\hat{V} = (\check{U} + i\check{V})(\check{\varphi} + i\check{\psi})\, e^{1/2i\int_0^{\Delta l}(\Delta l - l)(A_1U - A_2V)\, dl}, \tag{11}$$
$$\hat{\varphi} + i\hat{\psi} = (\check{\varphi} + i\check{\psi})\, e^{1/2i\,\Delta l\int_0^{\Delta l}(A_1U - A_2V)}. \tag{12}$$

Next we calculate approximately the right-hand side integrals of (11) and (12), so that both (11) and (12) will be fourth-order accurate relationships. In other words, we must calculate the integral in (11) with an accuracy $O(\Delta l^4)$ and the integral in (12) with an accuracy $O(\Delta l^3)$. For this purpose, in the first case we use a linear interpolation of the function $(A_1 U - A_2 V)$ and in the second, we apply the trapezoid rule,

$$
\begin{aligned}
I_1 &= \int_0^{\Delta l} (\Delta l - l)(A_1 U - A_2 V)\, dl \\
&= \int_0^{\Delta l} (\Delta l - l) \left\{ \left[ (\hat{A}_1 \hat{U} - \hat{A}_2 \hat{V}) \frac{l}{\Delta l} \right.\right. \\
&\quad \left.\left. + (\check{A}_1 \check{U} - \check{A}_2 \check{V}) \left(1 - \frac{l}{\Delta l}\right) \right] + O(\Delta l^2) \right\} dl \\
&= \frac{\Delta l^2}{6} [(\hat{A}_1 \hat{U} - \hat{A}_2 \hat{V}) + 2(\check{A}_1 \check{U} - \check{A}_2 \check{V})] + O(\Delta l^4), \\
I_2 &= \int_0^{\Delta l} (A_1 U - A_2 V)\, dl = \frac{\Delta l}{2} [(\hat{A}_1 \hat{U} - \hat{A}_2 \hat{V}) + (\check{A}_1 \check{U} - \check{A}_2 \check{V})] + O(\Delta l^3).
\end{aligned}
$$

Then

$$
e^{i(1/2)I_1} = 1 + \frac{\Delta l^2}{12} i[2(\check{A}_1 \check{U} - \check{A}_2 \check{V}) + (\hat{A}_1 \hat{U} - \hat{A}_2 \hat{V})] + O(\Delta l^4),
$$

$$
e^{i(1/2)I_2 \Delta l} = 1 + \frac{\Delta l^2}{4} i[(\check{A}_1 \check{U} - \check{A}_2 \check{V}) + (\hat{A}_1 \hat{U} - \hat{A}_2 \hat{V})] + O(\Delta l^4)
$$

and

$$
\begin{aligned}
\hat{U} + i\hat{V} &= (\check{U} + i\check{V})(\check{\phi} + i\check{\psi}) \left\{ 1 + \frac{\Delta l^2}{12} i[2(\check{A}_1 \check{U} - \check{A}_2 \check{V}) \right. \\
&\qquad \left. + (\hat{A}_1 \hat{U} - \hat{A}_2 \hat{V})] + O(\Delta l^4) \right\}, \\
\hat{\phi} + i\hat{\psi} &= (\check{\phi} + i\check{\psi}) \left\{ 1 + \frac{\Delta l^2}{4} i[(\check{A}_1 \check{U} - \check{A}_2 \check{V}) + (\hat{A}_1 \hat{U} - \hat{A}_2 \hat{V})] + O(\Delta l^4) \right\}.
\end{aligned}
$$

Introducing new designations

$$
\begin{aligned}
c + id &= (\check{U} + i\check{V})(\check{\phi} + i\check{\psi}), \\
\Delta L &= \frac{\Delta l^2}{12}, \\
F &= A_1 U - A_2 V,
\end{aligned}
$$

we obtain

$$
\begin{aligned}
(1 + d\,\Delta L\hat{A}_1)\,\hat{U} - d\,\Delta L\hat{A}_2\,\hat{V} &= c - d\,\Delta L 2\check{F} + O(\Delta l^4),\\
-c\,\Delta L\hat{A}_1\,\hat{U} + (1 + c\,\Delta L\hat{A}_2)\,\hat{V} &= d + c\,\Delta L 2\check{F} + O(\Delta l^4),\\
\hat{\varphi} &= \check{\varphi} - 3\Delta L\check{\psi}(\check{F} + \hat{F}) + O(\Delta l^4),\\
\hat{\psi} &= \check{\psi} + 3\Delta L\check{\varphi}(\check{F} + \hat{F}) + O(\Delta l^4),
\end{aligned}
$$

which, if we omit the fourth-order small terms, yields

$$
\begin{aligned}
\hat{U} &= \frac{1}{\det}\,[c + \Delta L(\hat{A}_2 - 2d\check{F})],\\
\hat{V} &= \frac{1}{\det}\,[d + \Delta L(\hat{A}_1 + 2c\check{F})],
\end{aligned}
\tag{13}
$$

where

$$
\det = 1 + \Delta L(c\hat{A}_2 + d\hat{A}_1). \tag{14}
$$

Note that

$$
\hat{U}^2 + \hat{V}^2 = \frac{1 + 2\Delta L(c\hat{A}_2 + d\hat{A}_1) + O(\Delta l^4)}{\det^2} = 1 + O(\Delta l^4),
$$

i.e., the obtained solution with an accuracy $O(l^4)$ satisfies the relationship

$$
U^2 + V^2 = 1 \tag{15}
$$

which must be exactly fulfilled due to the substitution (10*a*). Step-by-step accumulation of such an error may lead to the instability. To avoid this, we propose the following procedure of solution correction, which provides a more precise solution exactly satisfying relationship (15).

The idea of the procedure suggested is clearly illustrated by Fig. 2; in the plane $U$, $V$ we return the point to a unit circle along the radius vector. It is evident that thereby we only approach the calculated solution to the exact one.

The point return to the circle is described by the formulas

$$
\hat{U}_n = \frac{\hat{U}}{\sqrt{\hat{U}^2 + \hat{V}^2}}, \qquad \hat{V}_n = \frac{\hat{V}}{\sqrt{\hat{U}^2 + \hat{V}^2}} \tag{16}
$$

which yield

$$
\hat{U}_n^2 + \hat{V}_n^2 \equiv 1. \tag{17}
$$

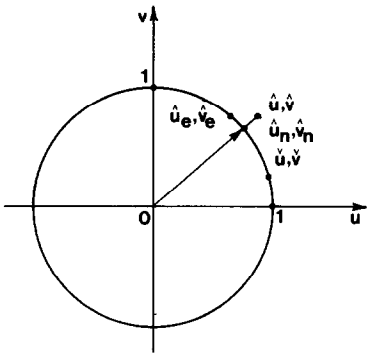


FIG. 2. A solution correction procedure for the electron motion equation. $\check{U}$, $\check{V}$ are the initial values; $\hat{U}$, $\hat{V}$ noncorrected values, $\hat{U}_n$, $\hat{V}_n$ corrected values; $\hat{U}_e$, $\hat{V}_e$ exact values at the calculated point.

It can be also easily shown that

$$\hat{U}_n = \hat{U} + O(\Delta l^4), \qquad \hat{V}_n = \hat{V} + O(\Delta l^4).$$

To find $\hat{U}_n$, $\hat{V}_n$, it is not necessary to calculate the value of det (14) and perform division in formulas (13).

Doing the same with $\varphi$ and $\psi$ variables, we obtain

$$\hat{\varphi}_n = \frac{\hat{\varphi}}{\sqrt{\hat{\varphi}^2 + \hat{\psi}^2}}, \qquad \hat{\psi}_n = \frac{\hat{\psi}}{\sqrt{\hat{\varphi}^2 + \hat{\psi}^2}},$$

and

$$\hat{\varphi}_n^2 + \hat{\psi}_n^2 \equiv 1. \tag{18}$$

Note that together with integrals (17) and (18) the following relations take place:

$$c^2 + d^2 \equiv 1,$$

$$I_1 = c\hat{U}_n + d\hat{V}_n = 1 - |O(\Delta l^4)|, \tag{19a}$$

$$I_2 = d\hat{U}_n - c\hat{V}_n = O(\Delta l^2). \tag{19b}$$

Moreover, two last relations can be used to check the correctness of the calculations.

Having solved Eq. (2) (i.e., the solutions of $N \times N_1$ independent ordinary differential equations such as (7)), it is easy to calculate the values $I = (1/2\pi)\int_0^{2\pi} e^{-i\theta}\, d\theta_0$ and $B = \int_0^L I\, dz$ by the known formulas of numerical integration.

## 4. Numerical Integration of the Equation for the Wave

When passing from the curent time level to the next one we wished to design a scheme of a rather high order of accuracy. But the values $B = \int_0^L I\,dz$ in the right-hand side of Eq. (1) (or (5)) are known only at the current level. Three-level schemes seem to be useful to reconcile our wishes and possibilities.

In paper [11] the three-level scheme stable for $\Delta\tau \leqslant h$ ($\Delta\tau$ is the time step) suggested in [12] was used to solve an equation similar to (5). However, that scheme is only second-order accurate in time. In our opinion, the integration along the characteristics is more natural and simple. If we integrate Eq. (5) along its characteristics $\xi = x + \varepsilon\tau$, then Eqs. (5) and (1) become practically the same. The only difference is that in the case of stationary electron injection, the direction of characteristics coincides with the direction of $\tau$ variable and it is possible to ignore the strict relation between mesh size in the $x$ coordinate and time step. Therefore, all further reasoning will concern only Eq. (1), while for Eq. (5) we shall give the final results and pay attention to some details.

The substitution $E = Ae^{\tau}$ transforms Eq. (1) to the equation $\dot{E} = Be^{\tau}$ (the point denotes differentiation with respect to the characteristic of the equation for the wave).

One of the possible third-order accurate schemes is obtained as follows

$$
\begin{aligned}
E_{n+1} &= E_n + \int_0^{\Delta\tau} Be^{\tau}\,d\tau = E_n + \int_0^{\Delta\tau} \left[B_n + \dot{B}_n\tau + \ddot{B}(\theta_1)\frac{\tau^2}{2}\right] e^{\tau}\,d\tau \\
&= E_n + B_n(e^{\Delta\tau} - 1) + \int_0^{\Delta\tau} \left[\frac{B_n - B_{n-1}}{\Delta\tau} + \ddot{B}(\theta_2)\frac{\Delta\tau}{2}\right] \tau e^{\tau}\,d\tau + \ddot{B}(\theta_1)\int_0^{\Delta\tau} \frac{\tau^2}{2} e^{\tau}\,d\tau \\
&= E_n + B_n(e^{\Delta\tau} - 1) + \frac{B_n - B_{n-1}}{\Delta\tau}(1 - e^{\Delta\tau} + \Delta\tau e^{\Delta\tau}) + O(\Delta\tau^3),
\end{aligned}
$$

where $n$ is the time level number. Neglecting the third-order small terms and returning to the $A$ variable we obtain the following computational scheme

$$
A_{n+1} = A_n e^{-\Delta\tau} + B_n\left[1 - \frac{(1 - \Delta\tau)(1 - e^{-\Delta\tau})}{\Delta\tau}\right] - B_{n-1}\left(1 - \frac{1 - e^{-\Delta\tau}}{\Delta\tau}\right). \quad (20)
$$

The truncation error for this scheme is equal to

$$
\varepsilon_1 = \tfrac{5}{12}(\ddot{A}_n + \dddot{A}_n)\,\Delta\tau^3 + O(\Delta\tau^4).
$$

To begin the computation, the following procedure is applied. Additional time levels are introduced between zero and first ones: the first additional level corresponds to $\tau = \Delta\tau/2^k$, the second one to $\tau = \Delta\tau/2^{k-1}$, etc. Calculation from the level $\tau = 0$ to the level $\tau = \Delta\tau/2^k$ can be performed using a two-level scheme, e.g.,

$$
A_{n+1} = A_n e^{-\Delta\tau/2^k} + B_n(1 - e^{-\Delta\tau/2^k}). \quad (21)
$$

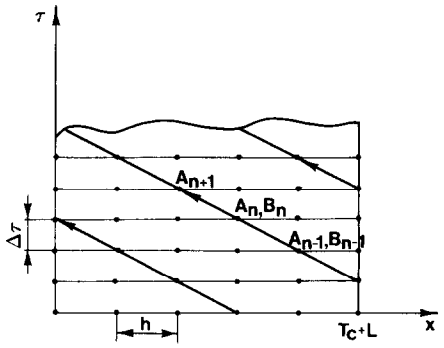


FIG. 3. A computational grid in the plane $x$, $\tau$ for integration of the equation for the wave in the case of pulse electron injection ($\Delta\tau = h/\varepsilon$, $\varepsilon = 2$).

In further calculations a three-level scheme is useful. Although the scheme (21) is only second-order accurate, it is possible to perform the first computational step with any necessary accuracy by choosing $k$ (in practice, the value $k \sim 3$ is sufficient).

Finally, we briefly consider the case of pulse electron injection. The scheme (20) is also applicable to Eq. (5). It is necessary only to keep the strict relation between $x$ mesh size and time step: $\Delta\tau = h/\varepsilon$ (Fig. 3). To begin the computation, the scheme (21) ($k = 0$) has been used. The second-order accuracy of this scheme is quite enough, since the characteristics starting from $\tau = 0$ level do not contribute essentially to the solution. An implicit third-order accurate scheme together with iterations

$$A_{n+1} = A_n e^{-\Delta\tau} + \frac{\Delta\tau}{2}(B_{n+1} + B_n e^{-\Delta\tau}) \tag{22}$$

gave the same results as the scheme (21).

The scheme (22) without iterations was used for executing the first computation from the line $x = T_c + L$. In place of $B_{n+1}$ a corresponding value of this function at the previous time level was taken. Note that in this case $A_n = 0$, $B_n = 0$ and (22) becomes

$$A_{n+1} = \frac{\Delta\tau}{2} B_{n+1}.$$

## 5. RESULTS

### *Analytical Test*

Let in Eqs. (2), (3), $\delta = 0$, and the wave amplitude small enough, i.e., $|A| \ll 1$. Then $\theta$ can be represented as

$$\theta = \theta_0 + \omega, \tag{23}$$

where $\theta_0$ is the solution of Eqs. (2)–(3) for $A \equiv 0$ and $\omega \ll 1$. Substituting (23) into (2), multiplying both sides of the equation obtained by $-(i/2\pi)\, e^{-i\theta_0}$, and integrating over the interval $\theta_0 \in [0, 2\pi]$ we have

$$-\frac{i}{2\pi}\left(\frac{\partial}{\partial x}+\frac{\partial}{\partial z}\right)^2 \int_0^{2\pi} \omega e^{-i\theta_0}\, d\theta_0$$

$$= -\frac{i}{2\pi}\int_0^{2\pi} e^{-i\theta_0} \cdot \frac{1}{2}\left[A e^{i(\theta_0+\omega)} + A^* e^{-i(\theta_0+\omega)}\right] d\theta_0,$$

where $A^*$ is the complex conjugate with respect to $A$. Linearizing both sides of the latter equation with respect to the state $A \equiv 0$, $\omega \equiv 0$, we arrive at

$$\left(\frac{\partial}{\partial x}+\frac{\partial}{\partial z}\right)^2 I = -\frac{iA}{2}. \tag{24}$$

TABLE I

The Solution of the Linearized Electron Motion Equation: $(\partial/\partial x + \partial/\partial z)^2 I = -iA/2$

| | $-\mathrm{Im}\left[B = \int_0^L g(x-z)\, I\, dz\right]$ | |
|---|---|---|
| $x$ | Analytical | Numerical |
| 0 | 0 | 0 |
| 0.4 | 0.0003 | 0.0003 |
| 0.8 | 0.0021 | 0.0021 |
| 1.2 | 0.0072 | 0.0072 |
| 1.6 | 0.0171 | 0.0171 |
| 2.0 | 0.0333 | 0.0334 |
| 2.4 | 0.0576 | 0.0576 |
| 2.8 | 0.0915 | 0.0914 |
| 3.2 | 0.1365 | 0.1362 |
| 3.6 | 0.1365 | 0.1362 |
| 4.0 | 0.1365 | 0.1362 |
| 4.4 | 0.1365 | 0.1362 |
| 4.8 | 0.1365 | 0.1362 |
| 5.2 | 0.1363 | 0.1359 |
| 5.6 | 0.1344 | 0.1340 |
| 6.0 | 0.1293 | 0.1290 |
| 6.4 | 0.1195 | 0.1191 |
| 6.8 | 0.1032 | 0.1028 |
| 7.2 | 0.0789 | 0.0786 |
| 7.6 | 0.0451 | 0.0448 |
| 8.0 | 0 | 0 |

*Notes.* $L = 3.2$, $T_c = 4.8$, $\delta = 0$, $N = 16$, $A = 0.05$, $h = 0.1$.

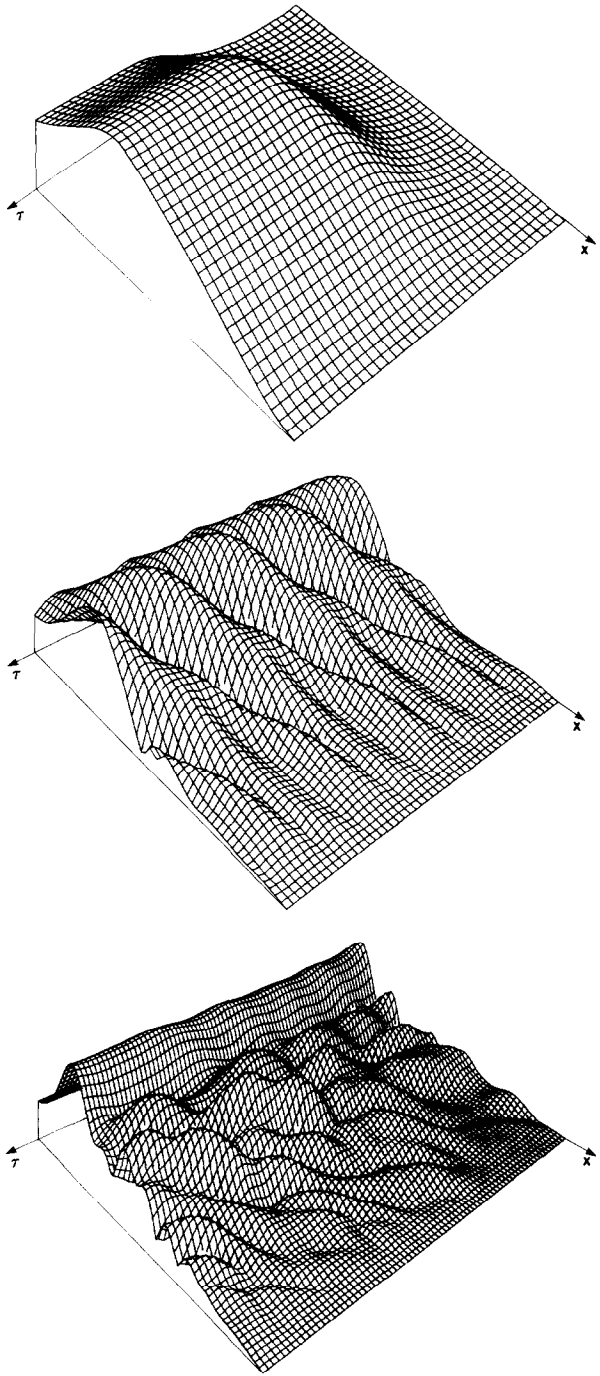


FIG. 4. Dynamics of the wave envelope structure in the case of pulse electron injection for various parameter values: (a) $L = 3$, $T_c = 5$, $N = 16$, $\varepsilon = 2.5$; (b) $L = 6.5$, $T_c = 5$, $N = 16$, $\varepsilon = 2.5$; (c) $L = 10$, $T_c = 6$, $N = 32$, $\varepsilon = 1$. In all cases $\delta = 0$, $h = 0.1$.

Now, if $A = \text{const}$, then

$$I = \frac{-iA}{4} z^2$$

and the function $B = \int_0^L I\,dz$ in the case of pulse injection is (assume, that $L \leqslant T_c$)

$$B(x) = -\frac{iAx^3}{12}, \qquad 0 \leqslant x \leqslant L,$$

$$= -\frac{iAL^3}{12}, \qquad L \leqslant x \leqslant T_c,$$

$$= -\frac{iA}{12}[L^3 - (x - T_c)^3], \qquad T_c \leqslant x \leqslant T_c + L.$$

Table I displays the results of this test.

TABLE II

Values of Integrals (19a) and (19b) for Various Regimes in FELs (the Case of Pulse Electron Injection)

| Point Number | | $I_1$ | $I_2$ | Point Number | | $I_1$ | $I_2$ |
|---|---|---|---|---|---|---|---|
| (a) | 0 | 1 | 0 | (c) | 0 | 1 | 0 |
| | 5 | 1 | −0.0016 | | 5 | 1 | −0.0010 |
| | 10 | 1 | −0.0003 | | 10 | 1 | 0.0005 |
| | 15 | 1 | 0.0014 | | 15 | 0.99999 | 0.0036 |
| | 20 | 0.99999 | 0.0032 | | 20 | 0.99998 | 0.0065 |
| | 25 | 0.99999 | 0.0042 | | 25 | 0.99999 | 0.0023 |
| | 30 | 1 | 0.0031 | | 30 | 0.99997 | −0.0073 |
| | | | | | 35 | 0.99998 | −0.0068 |
| (b) | 0 | 1 | 0 | | 40 | 1 | −0.0026 |
| | 5 | 1 | −0.0014 | | 45 | 1 | −0.0024 |
| | 10 | 1 | −0.0030 | | 50 | 0.99999 | −0.0043 |
| | 15 | 1 | −0.0043 | | 55 | 0.99999 | −0.0042 |
| | 20 | 0.99999 | −0.0053 | | 60 | 1 | −0.0019 |
| | 25 | 0.99999 | −0.0054 | | 65 | 1 | 0.0006 |
| | 30 | 0.99999 | −0.0039 | | 70 | 1 | 0.0006 |
| | 35 | 1 | −0.0008 | | 75 | 1 | −0.0021 |
| | 40 | 1 | 0.0015 | | 80 | 0.99999 | −0.0044 |
| | 45 | 1 | 0.0012 | | 85 | 1 | −0.0034 |
| | 50 | 1 | −0.0005 | | 90 | 1 | 0.0004 |
| | 55 | 1 | −0.0015 | | 95 | 1 | 0.0025 |
| | 60 | 1 | −0.0009 | | 100 | 1 | 0.0011 |
| | 65 | 1 | −0.0001 | | | | |

*Notes*: (a) $L = 3$, $T_c = 5$, $N = 16$, $\varepsilon = 2.5$; (b) $L = 6.5$, $T_c = 5$, $N = 16$, $\varepsilon = 2.5$; (c) $L = 10$, $T_c = 6$, $N = 32$, $\varepsilon = 1$.

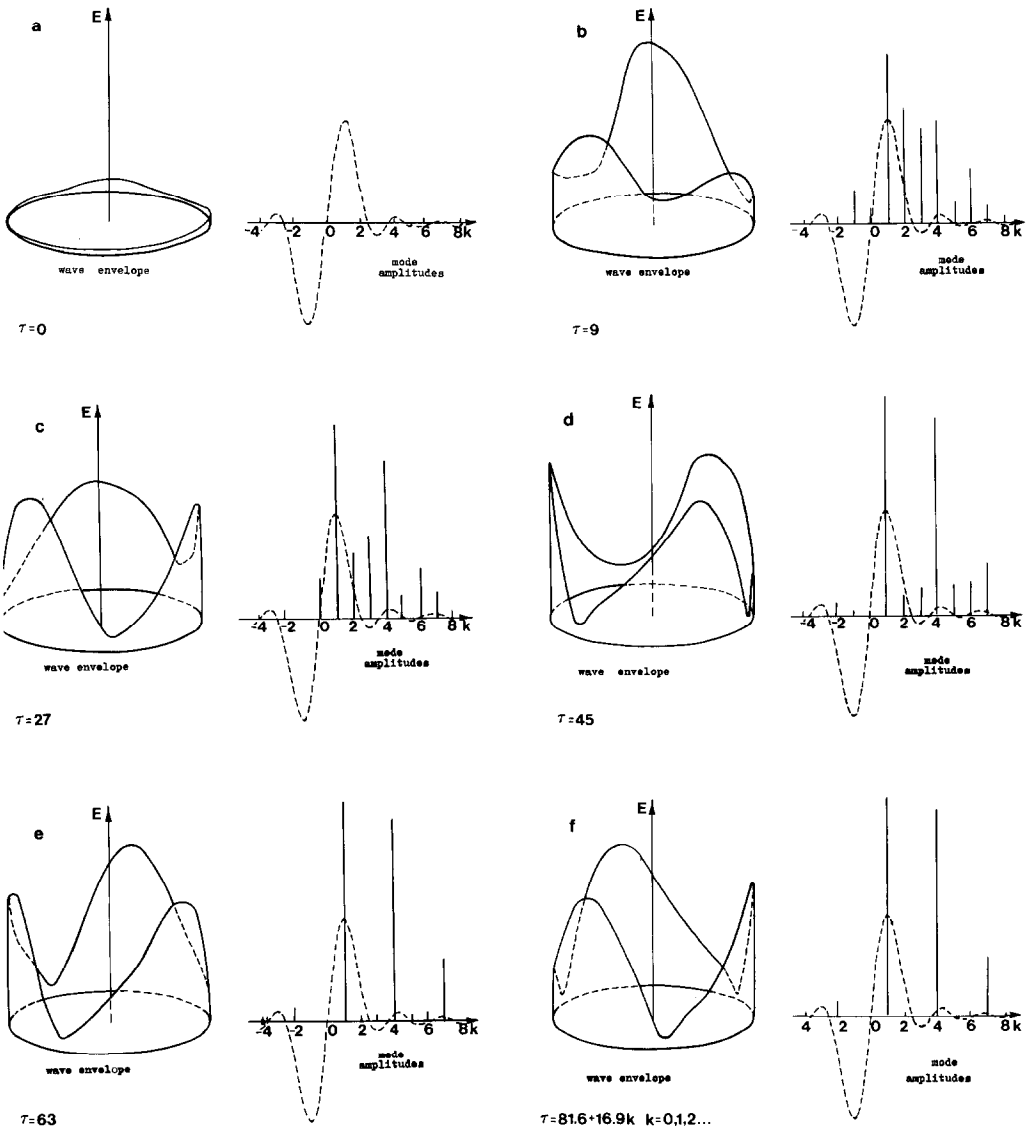


FIG. 5. (a)–(f) Periodic Automodulation. The frames from FEL film, demonstrating the evolution of the wave envelope and amplitudes of its harmonics in the case of stationary electron injection.

*Numerical Experiments*

The method based on the transition to the slow time and its numerical realization permitted to compute effectively the regimes of Stanford experiment [1] (generation of identical pulses), moreover, to advance considerably into the region of periodic and stochastic self-modulation regimes. And here an analogy with hydrodynamic problems is traced, when exceeding some threshold values of the injection current (an analogy with threshold values of the Reynolds number) three consecutive stages take place: (a) generation of identical pulses in the case of pulse electron injection or stationary single-mode generation in the case of stationary electron injection; (b) periodic; (c) stochastic self-modulation. Figs 4a, b and c displays the dynamics of the wave envelope structure in the case of pulse electron injection for different parameter values. Correspondingly, Tables IIa, b, c show a behavior of integrals (19a) and (19b) (see Sect. 3) at the fixed time level for some macroelectron with the same parameter values.

*Film*

Figure 5 displays some frames from an FEL film which demonstrates the evolution of the wave envelope and the amplitudes of its harmonics in the case of stationary electron injection. A periodic self-modulation regime calculated for the following parameter values: $L = 4.8$, $T_r = 12$, $\Delta\tau = 0.05$, $h = 0.1$, $N = 16$, $\delta = 0$, is shown.

Having performed 1632 computation steps ($\tau = 81.6$), all the amplitudes of harmonics become stationary, i.e., a certain structure of the wave envelope gyrated on a cylinder with gyration period $T_g = 16.9$ is established. The film has a frequency of one frame for every one computation step.

In conclusion we note that the scheme presented here can be easily modified in order to take into consideration the transverse boundedness of the wave field (formed because of diffraction) and the conjugate effect of the longitudinal diffusion of the wave packet (nonequidistance of the spectrum from the mode point of view) as well as tapering of the wiggler or uniform magnetic field and the dependence of the mirror reflection coefficients on the frequency.

## ACKNOWLEDGMENTS

The authors wish to express their gratitude to N. S. Ginzburg and M. I. Petelin for useful advice and discussions. We are also grateful to our referees for some reasonable remarks.

## REFERENCES

1. D. A. G. DEACON, L. R. ELIAS, J. M. MADEY, G. J. RAMIAN, H. A. SCHWETTMAN, AND T. I. SMITH, *Phys. Rev. Lett.* **38** (1977), 892.
2. G. DATTOLI AND A. RENIERI, *Lett. Nuovo Cimento* **24** (1979), 121.
3. H. AL-ABAWI, F. A. HOPF, G. T. MOORE, AND M. O. SCULLY, *Opt. Commun.* **30** (1979), 231.

4. F. A. HOPF, T. G. KUPER, G. T. MOORE, AND M. O. SCULLY, "Physics of Quantum Electronics" (S. F. Jacobs *et al.*, Eds.), Vol. 7, p. 31, Addison–Wesley. Reading, Mass., 1980.
5. T. G. KUPER, G. T. MOORE, AND M. O. SCULLY, *Opt. Commun.* **34** (1980), 117.
6. W. B. COLSON AND S. K. RIDE, "Physics of Quantum Electronics," (S. F. Jacobs *et al.*, Eds.), Vol. 7, p. 377, Addison–Wesley, Reading, Mass., 1980.
7. V. L. BRATMAN, N. S. GINZBURG, AND M. I. PETELIN, *Izv. Akad. Nauk. SSSR, Ser. Fiz.* **44** (1980), 1593.
8. YA. L. BOGOMOLOV, V. L. BRATMAN, N. S. GINZBURG, M. I. PETELIN, AND A. D. YUNAKOVSKY, *Opt. Commun.* **36** (1981), 209.
9. YA. L. BOGOMOLOV AND A. D. YUNAKOVSKY, Preprint No. 71, Institute of Applied Physics of the Academy of Sciences of the USSR, Gorky, USSR, 1983.
10. YA. L. BOGOMOLOV, N. S. GINZBURG, AND A. S. SERGEEV, Preprint No. 82, Institute of Applied Physics of the Academy of Sciences of the USSR, Gorky, USSR, 1983.
11. N. S. GINZBURG, S. P. KUZNETSOV, AND T. N. FEDOSEEVA, *Radiophys. Quantum Electron.*, January 1979, 728.
12. S. K. GODUNOV, "Equations of Mathematical Physics," p. 385, Nauka, Moscow, 1971.